

Disentangling chlorophyll fluorescence from atmospheric scattering effects in O₂ A-band spectra of reflected sun-light

C. Frankenberg,¹ A. Butz,² and G. C. Toon¹

Received 18 October 2010; revised 24 November 2010; accepted 13 December 2010; published 1 February 2011.

[1] Global retrieval of solar induced fluorescence emitted by terrestrial vegetation can provide an unprecedented measure for photosynthetic efficiency. The GOSAT (JAXA, launched Feb. 2009) and OCO-2 (NASA, to be launched 2013) satellites record high-resolution spectra in the O₂ A-band region, overlapping part of the chlorophyll fluorescence spectrum. We show that fluorescence cannot be unambiguously discriminated from atmospheric scattering effects using O₂ absorption lines. This can cause systematic biases in retrieved scattering parameters (aerosol optical thickness, aerosol height, surface pressure, surface albedo) if fluorescence is neglected. Hence, we demonstrate an efficient alternative fluorescence least-squares retrieval method based solely on strong Fraunhofer lines in the vicinity of the O₂ A-band, disentangling fluorescence from scattering effects. Not only does the Fraunhofer line fit produce a more accurate estimate of fluorescence emission, but it also allows improved retrievals of atmospheric aerosols from the O₂ A-band. **Citation:** Frankenberg, C., A. Butz, and G. C. Toon (2011), Disentangling chlorophyll fluorescence from atmospheric scattering effects in O₂ A-band spectra of reflected sun-light, *Geophys. Res. Lett.*, 38, L03801, doi:10.1029/2010GL045896.

1. Introduction

[2] Remote sensing of terrestrial vegetation is an important tool for monitoring its status and carbon flux estimation. From space, information is mainly based on indices such as the Normalized Difference Vegetation Index (NDVI), derived from hyper-spectral reflectance measurements in the visible to near-infrared spectral region. In the photosynthesis process, visible solar energy absorbed by chlorophyll can either be used for carbon fixation, be dissipated into heat, or be re-emitted via fluorescence at longer wavelengths. This so-called solar-induced chlorophyll fluorescence [Krause and Weis, 1991; Baker, 2008, and references therein] offers a more direct measure of photosynthetic activity. Its retrieval from space is the concept behind the scientific Fluorescence Explorer (FLEX) satellite mission, submitted to the European Space Agency (ESA) Earth Explorer program call in 2005.

[3] The fluorescence emission (F_s) adds a small offset of up to about $10 \text{ Wm}^{-2} \text{ sr}^{-1} \mu \text{ m}^{-1}$ [Entcheva Campbell et al., 2008] to the reflected solar spectrum over the 660–800 nm region with maxima at approximately 690 and 740 nm. This results in absorption lines appearing slightly shallower than otherwise. The fluorescence spectrum encompasses the

strongly saturated O₂A (around 765 nm) and the weaker B-band (around 685 nm). The small reduction in the fractional depths of O₂ and Fraunhofer absorption lines due to F_s is especially noticeable in saturated lines and can be used to retrieve fluorescence if spectra are recorded near the fluorescence source [Plascyk and Gabriel, 1975]. Meroni et al. [2009] provide a literature overview of common retrieval techniques for fluorescence signals, which are widely used for assessing photosynthetic activity [Krause and Weis, 1984, 1991; Flexas et al., 2002; Freedman et al., 2002; Zarco-Tejada et al., 2003; Moya et al., 2004; Rascher et al., 2009], including gross primary production (GPP) [Damm et al., 2010].

[4] Recent satellite missions aiming at measuring atmospheric abundances of carbon dioxide (CO₂) could enable retrievals of chlorophyll fluorescence as they feature high-resolution near-infrared spectrometers to record the O₂ A-band at $0.765 \mu \text{m}$. The Greenhouse Gases Observing Satellite (GOSAT) [Hamazaki et al., 2005; Kuze et al., 2009] was launched on 23 January 2009, while the Orbiting Carbon Observatory (OCO) [Crisp et al., 2004] suffered from a launch failure (launch of OCO-2 planned for early 2013).

[5] Guanter et al. [2010] provide the first study on the impact of aerosols on fluorescence retrievals and acknowledge potentially large errors, especially in the O₂ A-band. However, there is so far no study on I) the effect of fluorescence on the retrieval of scattering properties and II) on how to fully decouple the two effects in the absence of prior information on either. The goal of this paper is to bridge the gap between the vegetation and atmospheric communities by investigating the impact of scattering as well as fluorescence on high-resolution spectra. We will show that from spaceborne measurements of the O₂ A-band, fluorescence cannot be distinguished from the impacts of aerosols, albedo and surface pressure. However, we demonstrate a retrieval purely based on Fraunhofer lines outside the O₂ A-band, successfully isolating the fluorescence signal from scattering effects. We report the performance of the algorithm on the basis of simulated measurements according to GOSAT and OCO-2 specifications, paving the way towards space-based retrievals of chlorophyll fluorescence with current satellites.

2. The Retrieval Problem From Space

[6] Near the surface, fluorescence retrieval methods based on O₂ absorption lines work well since atmospheric scattering between the plants and the observer can be neglected and the atmospheric effect on the downwelling irradiance is normalized by means of measurements over reference panels located next to the canopy under study. In observations from space, as first performed by Guanter et al. [2007] using the MERIS imager with focus on a small region, the retrieval is

¹Jet Propulsion Laboratory, California Institute of Technology, Pasadena, California, USA.

²SRON Netherlands Institute for Space Research, Utrecht, Netherlands.

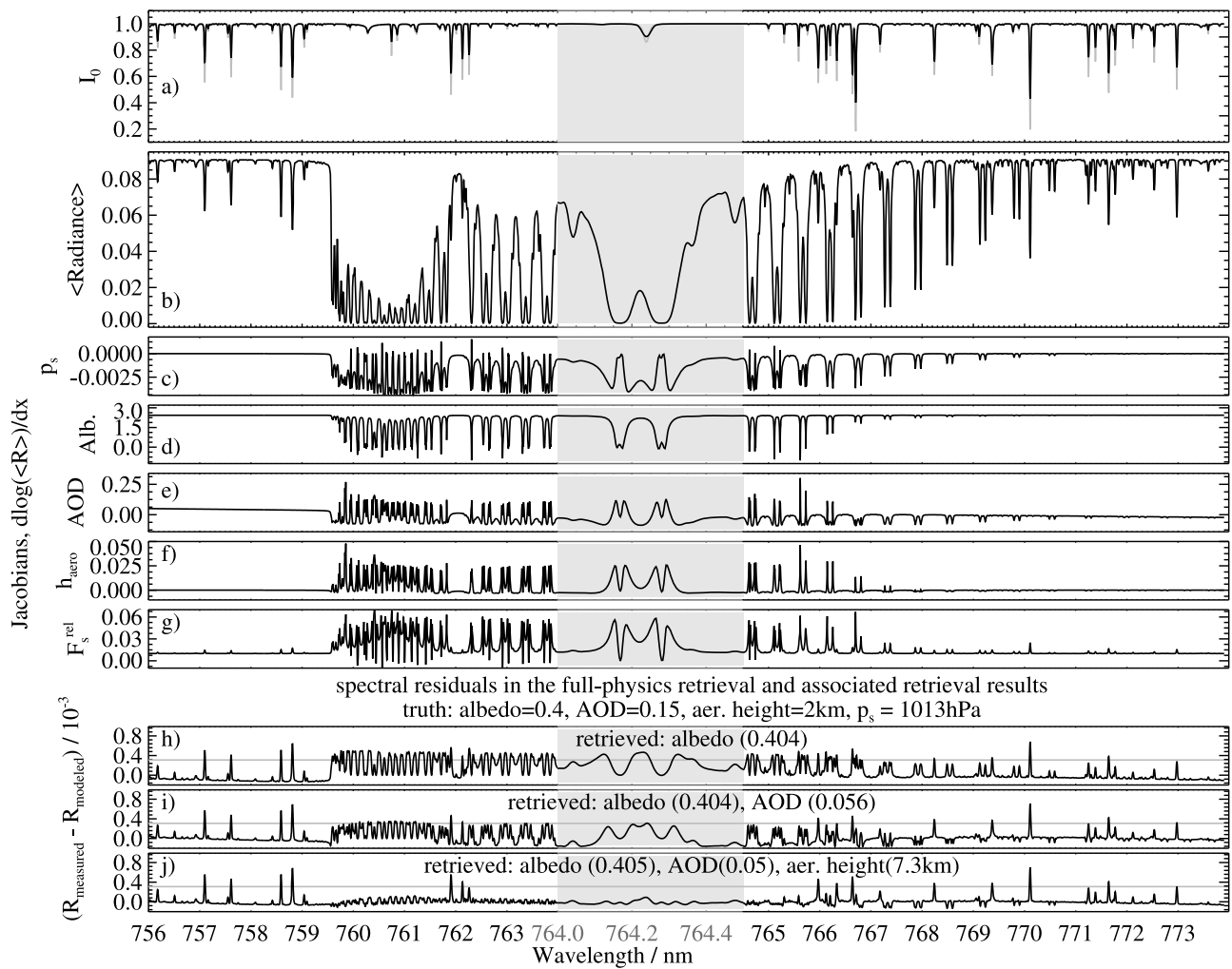


Figure 1. (a) Transmission spectrum of the incoming solar radiation, at full spectral resolution (gray, I_0) and convolved with a GOSAT instrument line shape (black, $\langle I_0 \rangle$). (b) Simulated backscatter spectrum R showing the strong O_2 A-band absorptions as observed from space (GOSAT instrumental line shape, solar zenith angle = 45° , exact nadir, aerosol optical depth at $765\text{ nm} = 0.15$, albedo = 0.4). (c–g) Jacobians ($\partial \log(R)/\partial x$) of the forward model with respect to surface pressure (p_s , in hPa), surface albedo (Alb.), aerosol optical depth (AOD), height of the a gaussian aerosol layer (in km) and additive fluorescence signal in terms of percentage of the continuum level (F_s^{rel}). The fluorescence Jacobian is calculated numerically. The gray-shaded area is a zoom on a narrow wavelength window to illustrate the effect on individual O_2 lines. (h–j) Spectral residuals as obtained from a full fit of a set of different parameters to a simulated spectrum (perturbed by a fluorescence offset of $\approx 1.5\%$). The gray horizontal lines in panels h–j indicate the level of measurement noise expected for a signal-to-noise ratio (SNR) = 300 .

more complicated. Even in the absence of aerosols, the fractional depths of the O_2 lines are not changed by the same amount as seen from ground since there is additional extinction of the fluorescence emission by O_2 between the surface and the top of atmosphere (TOA):

$$\vec{F}_s^{\text{TOA}} \approx \vec{F}_s^{\text{surface}} \cdot \exp(\mu_1 \cdot \vec{\tau}) \quad (1)$$

where \vec{F}_s are the fluorescence fluxes observed at the surface and TOA, $\vec{\tau}$ the vertically integrated optical density, μ_1 the secant of the viewing zenith angle (vectors are in wavelength space). Especially in the optically thick centers of the O_2 absorption lines (which provide the most distinctive signal at the surface level), F_s is completely absorbed at TOA.

[7] Even more importantly, elastic scattering processes due to aerosols and clouds alter the shape of recorded O_2

absorption lines in very similar ways to the fluorescence signal. In fact, high-resolution spectra of O_2 absorption lines are commonly used in atmospheric sciences to quantify scattering effects [Pfeilsticker *et al.*, 1998; Funk and Pfeilsticker, 2003; Bril *et al.*, 2007] while fluorescence is usually ignored. The prime objective of the O_2 A-band channels in GOSAT and OCO-2 is to derive those scattering properties of the atmosphere and thereby minimize the impact of aerosols and thin clouds on the retrieval of CO_2 , which is performed in additional channels covering CO_2 absorption bands at 1.61 and $2.06\ \mu\text{m}$ [Bösch *et al.*, 2006; Connor *et al.*, 2008; Oshchepkov *et al.*, 2008; Butz *et al.*, 2009; Reuter *et al.*, 2010].

[8] Owing to atomic absorptions in the sun's photosphere and chromosphere, the solar spectrum, as shown in Figure 1a, also exhibits narrow absorption lines, so-called Fraunhofer

lines (not to be confused with O₂ absorption lines). We use an empirical model of the disk-integrated solar transmission spectrum (continuum normalized to unity) to calculate the depths and shapes of the Fraunhofer absorption lines at full spectral resolution (see auxiliary material).¹

[9] To evaluate the impact of fluorescence on O₂ A-band retrievals, we perform a full-physics retrieval similar to *Butz et al.* [2009] with different choices of fitting parameters (aerosols, aerosol height, surface pressure, albedo). We use a linearized vector radiative transfer model [*Hasekamp and Landgraf*, 2002, 2005; *Hasekamp and Butz*, 2008] to efficiently compute radiances and Jacobians. Rotational Raman Scattering [*Grainger and Ring*, 1962; *Chance and Spurr*, 1997] is not considered in this study since at low solar zenith angles and relatively high surface albedos, the impact of Raman scattering is negligible [*Sioris and Evans*, 2000; *Sioris et al.*, 2003]. Similar considerations hold for inelastic scattering by particles [*Montagna and Dusi*, 1995; *Montagna*, 2008] but retrieval tests over regions with negligible fluorescence (e.g., deserts, fully cloudy pixels, ice/snow and ocean deserts) should be performed with real data to evaluate any impact of inelastic scattering processes.

[10] Figures 1b–1g show a simulated radiance and Jacobians at TOA for a typical atmospheric scenario at GOSAT spectral resolution (≈ 0.02 nm). It is obvious that the Jacobian with respect to fluorescence exhibits strong similarities with the other Jacobians in the O₂ lines but not in the Fraunhofer lines (e.g., at 758.8 or 770.1 nm).

[11] Figures 1h–1j show the effect of the neglect of an added wavelength-dependent fluorescence signal (see auxiliary material for details of the sensitivity study) on full-physics retrievals of scattering and surface properties. As expected from the shape of the Jacobians, fitting surface albedo, AOD and the height of the aerosol layer effectively mimics the impact of fluorescence in the O₂ lines, yielding spectral residuals well below typical measurement noise levels. Only the reduced fractional depths of Fraunhofer lines cannot be reproduced by the full-physics forward model, resulting in systematic residuals slightly above the noise level. If based only on O₂ lines, the Jacobians with respect to scattering properties and fluorescence are not linearly independent. A neglect of fluorescence thus leads to substantial systematic errors in other retrieved parameters without deteriorating the goodness of the least-squares fit. Fitting various combinations of atmospheric parameters, we find that neglecting F_s (on the order of 1–2%) causes substantial biases in surface albedo ($\Delta Alb. \approx 1\%$), AOD ($\Delta\tau \approx 0.1$), aerosol layer height ($\Delta h \approx 5$ km) and surface pressure ($\Delta p_s \approx 10$ hPa). This effect is non-trivial and strongly depends on the assumed scenario, forbidding a general statement of potential biases. As those errors will also propagate into greenhouse gas retrievals from space, when using the O₂ A-band to account for scattering, fluorescence must not be neglected.

3. Fraunhofer Line Fluorescence Retrieval Method

[12] Isolated Fraunhofer lines are affected only by fluorescence (not scattering) and allow for an unambiguous retrieval [*Plascyk and Gabriel*, 1975; *Corp et al.*, 2006]. Away from

O₂ absorption lines, there is no significant attenuation of the fluorescence signal emanating from the surface (in clear scenes) and we can greatly simplify the retrieval problem. A simple forward model \vec{f} for both continuum level variation (due to scattering and albedo variations) and fractional depth of Fraunhofer lines (changed only by fluorescence) reads

$$\vec{f}(F_s^{rel}, a) = \log(\langle \vec{I}_0 + F_s^{rel} \rangle) + \sum_{i=0}^n a_i \cdot \lambda^i, \quad (2)$$

where \vec{I}_0 is the high-resolution solar transmission spectrum, F_s^{rel} the relative fluorescence signal, the summation term an n 'th order polynomial describing the continuum radiance (similar to *Frankenberg et al.* [2005]). $\langle \rangle$ applies the convolution with the instrumental line-shape as well as the mapping of the high resolution model grid to the lower resolution spectrometer grid (see auxiliary material for details). As atmospheric scattering and surface albedo only affect the low-frequency behavior of the reflectance in the absence of telluric O₂ absorption lines, they can be efficiently characterized by the polynomial term, avoiding the need to run computationally expensive multiple-scattering radiative transfer calculations. Since we propose fairly small retrieval windows (a few nanometers wide), F_s^{rel} is assumed to be wavelength-independent, hence a scalar. A non-linear weighted least-squares algorithm provides the solutions for (F_s^{rel}, a) that minimize the Euclidian norm of the measurements-model difference vector (spectral residuals) inversely weighted by the respective 1σ noise estimates:

$$\arg \min \| S_e^{-1/2} (\vec{y} - \vec{f}(F_s^{rel}, a)) \|_2, \quad (3)$$

with \vec{y} being the measurement vector ($= \log(R(\vec{\lambda}))$) and S_e the strictly diagonal measurement error covariance matrix. In this setup (if I_0 is defined as transmission spectrum), F_s^{rel} is unit-less and the retrieved fluorescence flux F_s in radiance units can be approximated by $F_s = F_s^{rel} / (1 + F_s^{rel}) \cdot R_{cont}$.

[13] Focussing on spectral regions provided by GOSAT and OCO-2, there are two potential retrieval windows with sufficiently strong Fraunhofer lines. One is located at the short-wavelength side of the O₂ A-band around 757.5 nm, devoid of any telluric lines but covering 4 strong Fraunhofer lines (the strongest one at 758.81 nm with 44% transmission at full spectral resolution). The second window slightly overlaps weaker O₂ lines and ranges between 769.5 and 775 nm, covering the very strong potassium (K) I Fraunhofer line at 770.1 nm with slightly less than 20% transmission at full spectral resolution. *Joiner et al.* [2010] use this line for initial retrievals using GOSAT. In this latter window, O₂ absorption lines would have to be modeled as well, otherwise the unapodized sinc-type instrument function can cause retrieval interferences with O₂ lines. This can be done efficiently with, e.g., the IMAP-DOAS approach [*Frankenberg et al.*, 2005]. For the sake of simplicity, we focus on a retrieval sensitivity test using simulated noisy spectra in the former retrieval window (which is also closer to the fluorescence peak at 740 nm).

[14] Figure 2a shows a retrieval fitting a simulated spectrum with a 2.5% fluorescence signal and a SNR of 300 (Gaussian noise added). Small differences in spectral residuals (with/without fluorescence terms) are discernible. Figure 2b shows

¹Auxiliary materials are available in the HTML. doi:10.1029/2010GL045896.

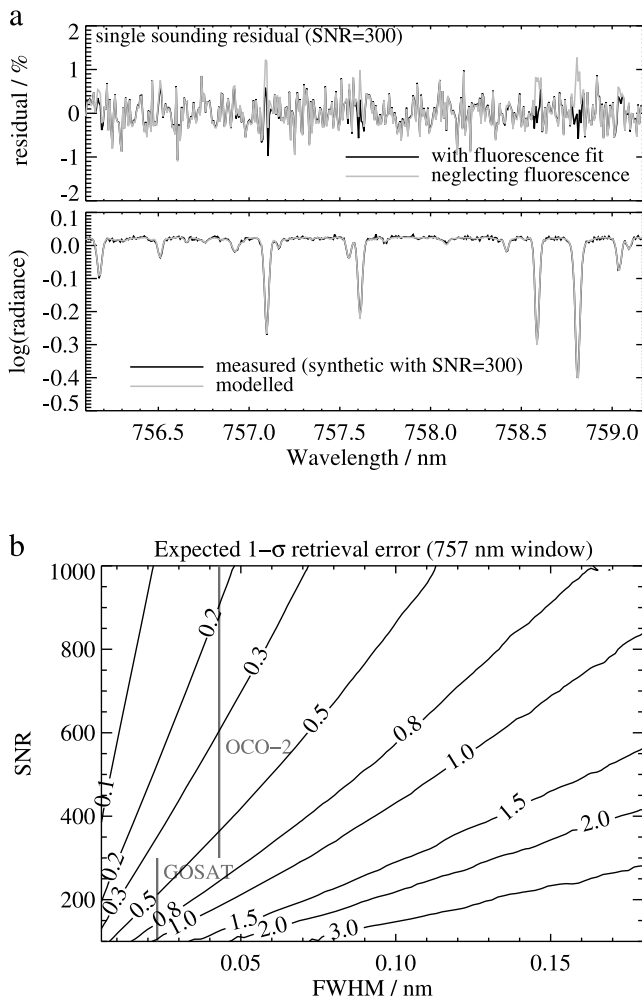


Figure 2. (a) (bottom) Fluorescence fit using Fraunhofer lines in the 757 nm region on a simulated spectrum with GOSAT instrumental line-shape, a 2.5% F_s^{rel} and SNR of 300. (top panel) Spectral residuals of a single fit (with and without accounting for potential fluorescence). (b) Contour plot of expected 1σ single measurement precision error in F_s^{rel} as a function of SNR and Full Width at Half Maximum (FWHM) of the instrumental line-shape. As in Figure 2a, the noise model represents a worst-case-scenario in which the absolute noise does not decrease within the absorption lines (justified for FTS-systems such as GOSAT but too conservative for grating spectrometers such as OCO-2). Typical FWHM and SNR ranges for GOSAT and OCO-2 are depicted as gray lines. Errors are given for F_s^{rel} as % of the continuum level radiance.

the expected precision error in F_s^{rel} as a function of SNR and FWHM (assuming 3 spectral samples per FWHM, see auxiliary material). Despite the lower spectral resolution of OCO-2, its higher SNR results in somewhat better precision when compared to GOSAT. Errors can be assumed random and do not exhibit any cross-correlation with scattering properties or surface albedo. Both GOSAT (with $\approx 10 \times 10 \text{ km}^2$ ground pixels) as well as OCO-2 (with $2 \times 2 \text{ km}^2$) therefore enable F_s retrievals from space. Their spatial resolution and revisit times will not yet allow for detailed local studies but both instruments have the potential to provide an

unprecedented proxy for carbon exchange on a global scale. In the future, high resolution spectra covering Fraunhofer lines at the short-wavelength side of the red-edge (720–740 nm) would be very advantageous since F_s is of similar magnitude but F_s^{rel} substantially larger due to lower surface albedo [Guanter et al., 2010].

[15] Instrumental effects such as stray-light (for a grating spectrometer such as OCO-2) or a zero-level offset (due to detector signal non-linearity [Abrams et al., 1994] in FTS systems such as GOSAT) also potentially fill in Fraunhofer lines and cannot be distinguished from the fluorescence signal. Ideally, these effects should be carefully calibrated prior to launch. Alternatively, they need to be properly characterized after launch, otherwise they might severely impede fluorescence retrievals from space.

4. Conclusions

[16] We analyzed the effect of solar-induced chlorophyll fluorescence on space-based nadir high resolution spectra of reflected sunlight in the O_2 A-band region. We showed that the effect of fluorescence on the shape of O_2 absorption lines cannot be unambiguously discriminated from the impact of atmospheric scattering properties as well as surface pressure and surface albedo. In fact, the neglect of fluorescence can cause substantial errors in the retrieval of scattering properties and vice versa, requiring an accurate independent prior estimate on one of those properties to avoid error cross-correlations in O_2 A-band retrievals.

[17] For an accurate retrieval of fluorescence from space, we proposed a computationally fast non-linear least squares algorithm exploiting strong Fraunhofer lines outside the O_2 A-band, decoupling fluorescence from scattering properties. We showed that with typical GOSAT and OCO-2 instrumental characteristics, the fluorescence signal can be retrieved with a single-measurement precision (1σ) of about 0.2–1% of the continuum level radiance. Both satellites were initially solely designed to gain, from a top-down perspective, deeper insight into the carbon budget by retrieving the global atmospheric CO_2 concentration. The additional retrieval of fluorescence is a) necessary in order to avoid retrieval biases in scattering properties and b) a unique additional proxy for photosynthetic activity, hence complementing information on the carbon budget from a bottom-up viewpoint.

[18] **Acknowledgments.** We thank O. Hasekamp and J. Landgraf from the SRON-Netherlands Institute for Space Research for kindly providing their radiative transfer code used in this study. The research described in this paper was carried out by the Jet Propulsion Laboratory, California Institute of Technology, under a contract with the National Aeronautics and Space Administration.

References

- Abrams, M., G. Toon, and R. Schindler (1994), Practical example of the correction of fourier-transform spectra for detector nonlinearity, *Appl. Opt.*, 33, 6307–6314.
- Baker, N. (2008), Chlorophyll fluorescence: A probe of photosynthesis in vivo, *Plant Biol.*, 59(1), 89.
- Bösch, H., et al. (2006), Space-based near-infrared CO_2 measurements: Testing the Orbiting Carbon Observatory retrieval algorithm and validation concept using SCIAMACHY observations over Park Falls, Wisconsin, *J. Geophys. Res.*, 111, D23302, doi:10.1029/2006JD007080.
- Bril, A., S. Oshchepkov, T. Yokota, and G. Inoue (2007), Parameterization of aerosol and cirrus cloud effects on reflected sunlight spectra measured

- from space: Application of the equivalence theorem, *Appl. Opt.*, **46**, 2460–2470.
- Butz, A., O. P. Hasekamp, C. Frankenberg, and I. Aben (2009), Retrievals of atmospheric CO₂ from simulated space-borne measurements of back-scattered near-infrared sunlight: Accounting for aerosol effects, *Appl. Opt.*, **48**, 3322–3336.
- Chance, K., and R. Spurr (1997), Ring effect studies: Rayleigh scattering, including molecular parameters for rotational raman scattering, and the Fraunhofer spectrum, *Appl. Opt.*, **36**, 5224–5230.
- Connor, B. J., H. Boesch, G. Toon, B. Sen, C. Miller, and D. Crisp (2008), Orbiting Carbon Observatory: Inverse method and prospective error analysis, *J. Geophys. Res.*, **113**, D05305, doi:10.1029/2006JD008336.
- Corp, L., E. Middleton, J. McMurtrey, P. E. Campbell, and L. Butcher (2006), Fluorescence sensing techniques for vegetation assessment, *Appl. Opt.*, **45**, 1023–1033.
- Crisp, D., et al. (2004), The Orbiting Carbon Observatory (OCO) mission, *Adv. Space Res.*, **34**(4), 700–709.
- Damm, A., et al. (2010), Remote sensing of sun-induced fluorescence to improve modeling of diurnal courses of gross primary production (GPP), *Global Change Biol.*, **16**(1), 171–186, doi:10.1111/j.1365-2486.2009.01908.x.
- Entcheva Campbell, P.-K., E.-M. Middleton, L.-A. Corp, and M.-S. Kim (2008), Contribution of chlorophyll fluorescence to the apparent vegetation reflectance, *Sci. Total Environ.*, **404**(2–3), 433–439.
- Flexas, J., J. Escalona, S. Evain, J. Gulias, I. Moya, C. Osmond, and H. Medrano (2002), Steady-state chlorophyll fluorescence (Fs) measurements as a tool to follow variations of net CO₂ assimilation and stomatal conductance during water-stress in C3 plants, *Physiol. Plant.*, **114**(2), 231–240.
- Frankenberg, C., U. Platt, and T. Wagner (2005), Iterative maximum a posteriori (IMAP)-DOAS for retrieval of strongly absorbing trace gases: Model studies for CH₄ and CO₂ retrieval from near infrared spectra of SCIAMACHY onboard ENVISAT, *Atmos. Chem. Phys.*, **5**, 9–22.
- Freedman, A., J. Cavender-Bares, P. Kebabian, R. Bhaskar, H. Scott, and F. Bazzaz (2002), Remote sensing of solar-excited plant fluorescence as a measure of photosynthetic rate, *Photosynthetica*, **40**(1), 127–132.
- Funk, O., and K. Pfeilsticker (2003), Photon path length distributions for cloudy skies? Oxygen A-band measurements and model calculations, *Ann. Geophys.*, **21**(3), 615–626.
- Grainger, J., and J. Ring (1962), Anomalous fraunhofer line profiles, *Nature*, **193**, 762.
- Guanter, L., L. Alonso, L. Gómez-Chova, J. Amorós-López, J. Vila, and J. Moreno (2007), Estimation of solar-induced vegetation fluorescence from space measurements, *Geophys. Res. Lett.*, **34**, L08401, doi:10.1029/2007GL029289.
- Guanter, L., L. Alonso, L. Gómez-Chova, M. Meroni, R. Preusker, J. Fischer, and J. Moreno (2010), Developments for vegetation fluorescence retrieval from spaceborne high-resolution spectrometry in the O₂-A and O₂-B absorption bands, *J. Geophys. Res.*, **115**, D19303, doi:10.1029/2009JD013716.
- Hamazaki, T., Y. Kaneko, A. Kuze, and K. Kondo (2005), Fourier transform spectrometer for Greenhouse Gases Observing Satellite (GOSAT), *Proc. SPIE*, **5659**, 73.
- Hasekamp, O. P., and A. Butz (2008), Efficient calculation of intensity and polarization spectra in vertically inhomogeneous scattering and absorbing atmospheres, *J. Geophys. Res.*, **113**, D20309, doi:10.1029/2008JD010379.
- Hasekamp, O., and J. Landgraf (2002), A linearized vector radiative transfer model for atmospheric trace gas retrieval, *J. Quant. Spectrosc. Radiat. Transfer*, **75**(2), 221–238.
- Hasekamp, O. P., and J. Landgraf (2005), Linearization of vector radiative transfer with respect to aerosol properties and its use in satellite remote sensing, *J. Geophys. Res.*, **110**, D04203, doi:10.1029/2004JD005260.
- Joiner, J., Y. Yoshida, A. Vasilkov, Y. Yoshida, L. Corp, and E. Middleton (2010), First observations of global and seasonal terrestrial chlorophyll fluorescence from space, *Biogeosci. Discuss.*, **7**(6), 8281–8318.
- Krause, G., and E. Weis (1984), Chlorophyll fluorescence as a tool in plant physiology, *Photosynth. Res.*, **5**(2), 139–157.
- Krause, G., and E. Weis (1991), Chlorophyll fluorescence and photosynthesis: The basics, *Annu. Rev. Plant Physiol. Plant Mol. Biol.*, **42**, 313–349.
- Kuze, A., H. Suto, M. Nakajima, and T. Hamazaki (2009), Thermal and near infrared sensor for carbon observation Fourier-transform spectrometer on the Greenhouse Gases Observing Satellite for greenhouse gases monitoring, *Appl. Opt.*, **48**, 6716–6733.
- Meroni, M., M. Rossini, L. Guanter, L. Alonso, U. Rascher, R. Colombo, and J. Moreno (2009), Remote sensing of solar-induced chlorophyll fluorescence: Review of methods and applications, *Remote Sens. Environ.*, **113**(10), 2037–2051, doi:10.1016/j.rse.2009.05.003.
- Montagna, M. (2008), Brillouin and raman scattering from the acoustic vibrations of spherical particles with a size comparable to the wavelength of the light, *Phys. Rev. B*, **77**(4), 045418, doi:10.1103/PhysRevB.77.045418.
- Montagna, M., and R. Dusi (1995), Raman scattering from small spherical particles, *Phys. Rev. B*, **52**(14), 10080, doi:10.1103/PhysRevB.52.10080.
- Moya, I., L. Camenen, S. Evain, Y. Goulas, Z. Cerovic, G. Latouche, J. Flexas, and A. Ounis (2004), A new instrument for passive remote sensing: 1. Measurements of sunlight-induced chlorophyll fluorescence, *Remote Sens. Environ.*, **91**(2), 186–197, doi:10.1016/j.rse.2004.02.012.
- Oshchepkov, S., A. Bril, and T. Yokota (2008), PPDF-based method to account for atmospheric light scattering in observations of carbon dioxide from space, *J. Geophys. Res.*, **113**, D23210, doi:10.1029/2008JD010061.
- Pfeilsticker, K., F. Erié, O. Funk, H. Veitel, and U. Platt (1998), First geometrical pathlengths probability density function derivation of the skylight from spectroscopically highly resolving oxygen A-band observations: 1. Measurement technique, atmospheric observations and model calculations, *J. Geophys. Res.*, **103**(D10), 11,483–11,504, doi:10.1029/98JD00725.
- Plascyk, J., and F. Gabriel (1975), The Fraunhofer line discriminator MKII—An airborne instrument for precise and standardized ecological luminescence measurement, *IEEE Trans. Instrum. Meas.*, **24**(4), 306–313.
- Rascher, U., et al. (2009), CEFLES2: The remote sensing component to quantify photosynthetic efficiency from the leaf to the region by measuring sun-induced fluorescence in the oxygen absorption bands, *Biogeosciences*, **6**(7), 1181–1198.
- Reuter, M., M. Buchwitz, O. Schneising, J. Heymann, H. Bovensmann, and J. P. Burrows (2010), A method for improved SCIAMACHY CO₂ retrieval in the presence of optically thin clouds, *Atmos. Meas. Tech.*, **3**(1), 209–232, doi:10.5194/amt-3-209-2010.
- Sioris, C. E., and W. F. J. Evans (2000), Impact of rotational Raman scattering in the O₂A band, *Geophys. Res. Lett.*, **27**(24), 4085–4088.
- Sioris, C. E., G. Bazalgette Courrèges-Lacoste, and M.-P. Stoll (2003), Filling in of Fraunhofer lines by plant fluorescence: Simulations for a nadir-viewing satellite-borne instrument, *J. Geophys. Res.*, **108**(D4), 4133, doi:10.1029/2001JD001321.
- Zarco-Tejada, P., J. Pushnik, S. Dobrowski, and S. Ustin (2003), Steady-state chlorophyll a fluorescence detection from canopy derivative reflectance and double-peak red-edge effects, *Remote Sens. Environ.*, **84**(2), 283–294.

A. Butz, SRON Netherlands Institute for Space Research, Sorbonnelaan 2, NL-3584 Utrecht, Netherlands.

C. Frankenberg and G. C. Toon, Jet Propulsion Laboratory, California Institute of Technology, 4800 Oak Grove Dr., Pasadena, CA 91109, USA. (christian.frankenberg@jpl.nasa.gov)